*Sensors & Transducers, Vol. 27, Special Issue, May 2014, pp. 92-99*

www.sensorsportal.com

**Sensors & Transducers**



*http://www.sensorsportal.com*

# Gold Electrodes Modified with Molecular Imprinted Acrylate Polymer for Impedimetric Determination of Testosterone

**Amina BETATACHE, Florence LAGARDE, Corinne SANGLAR, Anne BONHOMME, Didier LEONARD, Nicole JAFFREZIC-RENAULT**

University of Lyon, Institute of Analytical Sciences, UMR 5280 CNRS/UCBL/ENS,
5 rue de la Doua, 69100 Villeurbanne, France
Tel.: 33(0)437423558,
E-mail: nicole.jaffrezic@univ-lyon1.fr

*Received: 31 December 2012 /Accepted: 5 August 2013 /Published: 26 May 2014*

**Abstract:** A moleculary imprinted polymer (MIP) sensor was developed for impedimetric detection of testosterone. 4,4'-azobis(4-cyanovaleric acid) initiator was first grafted onto a gold electrode modified by a self-assembled monolayer of thiolamine (11-amino-1-undecanethiol). Methacrylic acid and ethylene glycol dimethacrylate were prepolymerized by photo-polymerization in presence of testosterone as template and then spincoated and polymerized on the functionalized electrode surface. The different steps of MIP sensor fabrication were controlled using electrochemical impedance spectroscopy (EIS), Fourier transform infrared spectroscopy and time of flight-secondary ion mass spectrometry. After template removal, the biosensor response, expressed as the variation of charge transfer resistance at the electrode/electrolyte interface measured by EIS, increased linearly with testosterone concentration up to 50 $\mu g.L^{-1}$. The sensitivity was 0.28 per log C for testosterone, while it was only 0.0085 and 0.020 for methyltestosterone and 17β-estradiol, respectively. A very good limit of detection (103 $ng.L^{-1}$) was achieved for testosterone. The sensitivity of the non imprinted polymer sensor, prepared the same way but in absence of template, was 18 times lower than that obtained with the MIP.


**Keywords:** Moleculary imprinted polymer, Testosterone, Electrochemical impedance spectroscopy, Cyclic voltammetry, TOF-SIMS, FTIR.

## 1. Introduction

Testosterone (T) is an endogenous steroid hormone with strong androgenic and anabolic effects. Important functions such as pubertal development, bone density or muscle mass are known to be influenced by T. Although the use of anabolic substances to enhance the athletic performance has been banned since several decades by the International Olympic Committee and T has been included in the List of Prohibited Substances edited by the World Antidoping Agency [1], this substance still remains one of the most frequent molecules reported in steroid misuse in sport.

A number of methods have been reported for T detection in human samples including blood [2-7], urine [8-11], hair [12] or saliva [6, 13-14]. Immunoassays are generally methods of choice for

clinical routine analysis. However, classical T assays suffer from insufficient sensitivity and specificity, resulting in an overestimation of T concentrations in the low range [15-16]. Chromatographic techniques, involving HPLC [9-10] or GC [10] or a combination of both [8-9] coupled with mass spectrometric (MS) detection, are becoming the analytical methods of choice over immunoassays due to their high specificity and accuracy. However, they are time-consuming, expensive and generally require tedious pre-treatment procedures such as liquid–liquid extraction, solid phase extraction or derivatization steps. These techniques may be also considered as harmful for environment as they use large amounts of volatile organic solvents.

Several electrochemical immunosensors using horseradish peroxidase (HRP) labelling have therefore been developed for rapid, selective and inexpensive detection of T [5-6, 11, 17]. A label-free potentiometric immunosensor based on gold nanowires has been also reported [7]. The main limitation of immunosensor technology is related to the high cost and poor stability of antibodies used as bioreceptors. Due to their relatively inexpensive and easy way of preparation, their mechanical and chemical stability, moleculary imprinted polymers (MIPs) have been claimed as possible substitutes for immunological material in chemical sensor. MIP allows the construction of tailor-made binding sites for a given target or a group of target molecules [18]. Most of MIPs are synthetized through a free radical polymerization process, induced either thermally or photochemically [19]. A functional monomer and an excess of cross-linker are polymerized in presence of the target molecule (template). Then, the template is removed from the cross-linked polymer network to leave functional recognition sites with a shape that is complementary to the template. MIPs have been used in a variety of applications, including separation sciences and purification, sensors and biosensors, catalysis and drug delivery [18].

Several MIPs have been developed for specific recognition of T, but they have been used principally for the elaboration of separation or pre-concentration supports [20-24]. To the best of our knowledge, only one MIP based sensor for SPR detection of T has been previously reported [25].

In this work, we propose the first MIP based sensor for T electrochemical detection. Prior to polymerization, 4,4'-azobis(4-cyanovaleric acid) photoinitiator was covalently coupled to a self-assembled monolayer of amine terminated alkanethiol grafted onto a gold electrode. The same approach had been already used by Lotierzo et al for the development of a surface plasmon resonance sensor for domoic acid determination [26]. The different steps of sensor fabrication were characterized using electrochemical impedance spectroscopy (EIS) and Time of flight-secondary ion mass spectrometry (TOF-SIMS). Methacrylic acid (MA) and ethylene glycol dimethacrylate (EGDMA) were prepolymerized by photo-polymerization in presence of testosterone as template and then casted and polymerized on the functionalized electrode surface. Surface polymerization and T removal were monitored using Fourier transformed infrared spectroscopy (IRTF). EIS and cyclic voltammetry (CV) responses of the MIP sensor were measured at different T concentrations and analytical features of the MIP sensor were determined.

## 2. Materials and Methods

### 2.1. Reagents

11-amino-1-undecanethiol hydrochloride (AUT, 99 %), 4,4'-azobis (4-cyanovaleric acid) (ACVA, >98 %), 1-hydroxybenzotriazole (HOBt, >99 %), ethylene glycol dimethacrylate (98 %), methacrylic acid (99 %), N-(3-dimethylaminopropyl)-N'-ethylcarbodiimide hydrochloride (protein seq grade) (EDC), Testosterone (>99 %) and 2,2'-azobis(2-methyl-propionitrile) (AIBN, 98 %), N,N-dimethyl-formamide (DMF, 99.8 %), methanol (99,8 %), $K_3Fe(CN)_6$ (>99 %), $K_4Fe(CN)_6 \cdot 3H_2O$ (98.5-102 %) and phosphate buffered saline (PBS) tablets were purchased from Sigma-Aldrich and used as received. All reagents were of analytical grade and ultra-pure water (resistivity 18.2 MΩ.cm) was used for all experiments.

### 2.2. MIP-Sensor

The MIP-sensor is shown in Fig.1. Gold substrates were fabricated by LAAS-RTB platform (CNRS Toulouse) using standard silicon technologies. (100)-oriented, P-type (3-5 ohm cm) silicon wafer was thermally oxidized to grow an 800 nm thick field oxide. Then, a 30 nm-thick titanium layer followed by a 300 nm-thick gold top layer was deposited by evaporation under vacuum. The bare gold electrodes were first cleaned with acetone in ultrasonic bath for 15 min, then with freshly prepared "piranha" solution (70 % $H_2SO_4$, 30 % $H_2O_2$) for 5 min, rinsed with ultrapure water and then with ethanol. After each treatment, gold electrodes were dried under nitrogen flow.

Then, the gold electrodes were coated with a self-assembled monolayer by incubation in 1 mM AUT ethanol solution for 24 h at room temperature, cleaned with water and ethanol, and dried under nitrogen flow.

A solution containing 20 mM ACVA photo-initiator, 20 mM water-soluble EDC and 20mM HOBt in DMF was allowed to stand for 1 h in order to activate ACVA carboxylic groups. Then, the amino-functionalised gold surface was contacted for 16 h in the dark with the former solution to bind ACVA to the surface. After that, a 1:8 T:MA mixture was prepared in DMF, purged with nitrogen for

15 min, and allowed to stand to form T-MA complex. EGDMA cross-linker (1:25 T:EGDMA proportion) as well as 4 % wt of AIBN (used as co-initiator) were then added to this solution, and this prepolymerisation mixture was activated by UV light for 1 min to increase the solution viscosity. The resulting solution was spin-coated on the gold electrode (previously washed with DMF and dried under nitrogen) to obtain a homogenous layer.

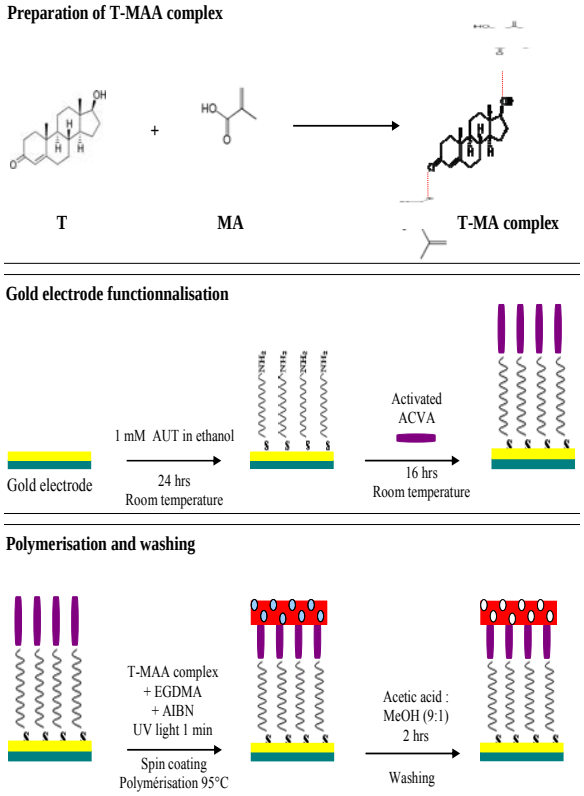


**Fig. 1.** MIP-sensor fabrication using a surface-bound photo-radical initiator.

The sensor was placed for 96 min in an Ivoclar Targis Power light curing unit (visible, T = 95 °C) for polymerization. Afterwards, the MIP-sensor was incubated in a 9:1 methanol: acetic acid mixture for 2 hrs to remove testosterone. Another gold electrode was prepared following the same procedure but without the testosterone template to fabricate a non-imprinted polymer (NIP) sensor.

## 2.3. Instrumentation

Electrochemical equipment.

Electrochemical measurements were carried out in PBS buffer containing 5 mM ferri/ferrocyanide using a VoltaLab 80 instrument equipped with a PGZ 402 potentiostat and controlled with Voltamaster 4.0 software. A three electrode device, including the modified gold electrode as working electrode (active area: 0.071 $cm^2$), a saturated calomel electrode (SCE) as the reference electrode and a platinum plate (0.19 $cm^2$) as counter electrode, was used.

Impedance measurements were carried out in the 100 mHz-100 kHz frequency range, under a dc potential of -400 mV. Cyclic voltammetry measurements were performed at a scanning rate of 100 $mV.cm^{-1}$.

FTIR spectroscopy.

Infrared spectra were recorded at room temperature using a Nicolet Continuµm infrared microscope working in attenuated total reflectance in monoreflexion with a germanium crystal. Spectral width and resolution were 650-4000 $cm^{-1}$ and 4 $cm^{-1}$, respectively. Data processing was performed using Happ-Genzel apodization (256 scans).

TOF-SIMS.

Measurements were carried out at Université Claude Bernard-Lyon 1 (Villeurbanne, France) using a Physical Electronics TRIFT III ToF-SIMS instrument (Physical Electronics, Chanhassen, USA) operated with a pulsed 22 keV Au+ ion gun (ion current of 2 nA) rastered over a 300 µm x 300 µm. Data were analyzed using the WinCadenceTM software. Mass calibration was performed on hydrocarbon secondary ions together with Au+/-.

# 3. Results and Discussion

## 3.1. Control of the MIP Sensor Fabrication

Characterization of SAM and SAM/ACVA modified gold electrodes EIS.

Complex impedance spectra (Nyquist plots) of bare Au, Au/SAM and Au/SAM/ACVA electrodes were recorded in PBS containing 5 mM ferro/ferricyanide ions. As seen in Fig. 2, complex impedance increased by grafting the different layers on the electrode.

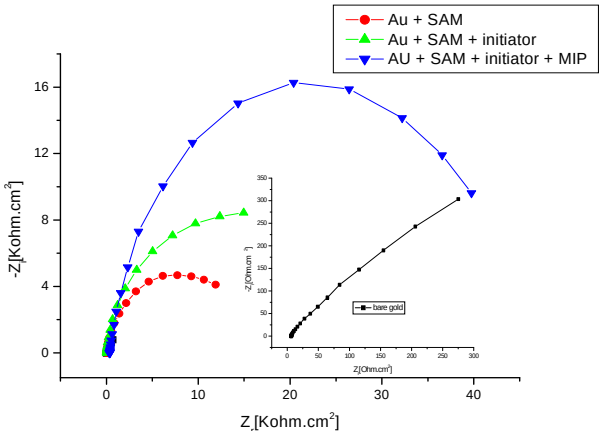


**Fig. 2.** Complex impedance spectra (Nyquist plots) of bare Au (insert) and of the electrode after grafting the different layers described in Fig. 1. EIS measurements were performed at -400 mV in 5 mM ferro/ferricyanide PBS buffer.

All spectra could be satisfactorily fitted with the classical Randles equivalent electrical circuit using Zview software. The model includes two resistive elements, $R_S$ and $R_{ct}$, and CPE, a constant phase angle element (Fig. 3). $R_S$ corresponds to the ohmic resistance of the bulk electrolyte and $R_{ct}$ to the charge transfer resistance between the solution and the modified electrode surface. $R_{ct}$ values obtained from modelling were respectively 3.8, 16.3 and 25.5 kΩ.cm$^2$.

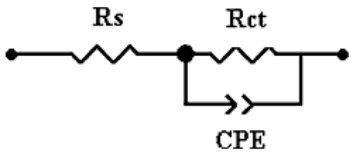


**Fig. 3.** Equivalent electrical circuit used for impedance spectra modelling.

They were used to calculate the electrode coverage rate after SAM and SAM/ACVA modifications according to Eq. 1.

$$\Theta = 1 - \frac{R_{ct}^{Au}}{R_{ct}^{SAM}}, \quad (1)$$

where $R_{ct}^{Au}$ and $R_{ct}^{SAM}$ are the charge transfer resistances for bare Au and for Au/SAM electrodes, respectively.

The coverage rate was 0.76 after SAM modification and 0.84 after ACVA fixation, showing a densification of the layer after initiator grafting.

TOF-SIMS

Fig. 4 displays TOF-SIMS spectra recorded in negative mode in the 3-30 m/z range. The peak observed for m/z = 26.004 on the bare electrode spectrum was attributed to CN groups (calculated value: 26.003). A peak at m/ z = 26.003 and 26.004 was also obtained for the Au/SAM and Au/SAM/ACVA electrodes, respectively.

The bare gold exhibited a slight relative intensity for the signatures related to nitrogen such as CN. The relative intensity increased after grafting the thiolamine SAM onto the electrode, and increased again by additional fixation of ACVA initiator. Considering the structures of thiolamine and initiator, the relative intensities correspond fairly well.

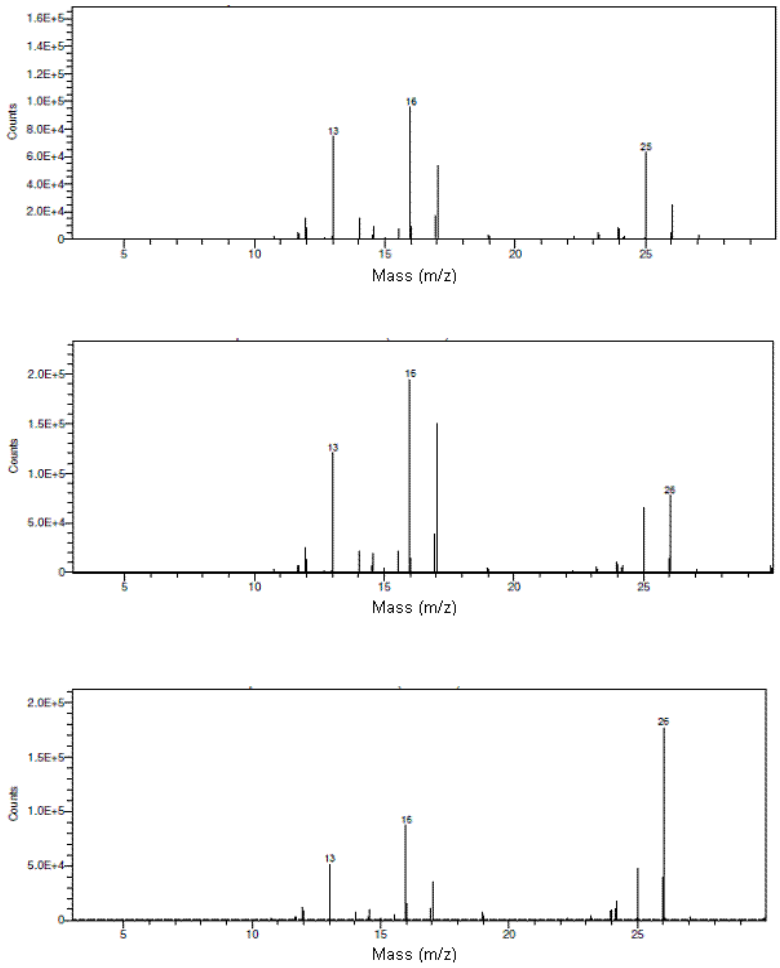


**Fig. 4.** TOF-SIMS negative mode spectra of the bare (a), the thiolamine modified (b) and the thiolamine/initiator modified (c) electrodes.

MIP film characterization

EIS

Nyquist diagram obtained after deposition and polymerization of the prepolymerization mixture is presented in Fig. 2. $R_{ct}$ value after polymerization was about twice that observed for the Au/SAM/ACVA electrode, showing the formation of a dense polymerized insulating film at the electrode surface.

IRTF

FTIR spectroscopy was used to assess polymerization efficiency after deposition of the prepolymer mixture on the SAM/ACVA modified electrode and to characterize chemical properties of the synthetized MIP film.

Fig. 5 compares IRTF spectrum of the prepolymerization mixture without template (EGDMA+MA) with that of the NIP film obtained after polymerization. NIP film synthesis was confirmed by the disappearance of the carbon double bond vibration peak (υ C=C) at 1636 $cm^{-1}$.

IRTF spectroscopy was also used to evaluate the efficiency of methanol/acetic acid washing procedure used to remove T template from the MIP after polymerization. The peak detected at 1661 $cm^{-1}$ in Fig. 6b may be assigned to the carbonyl vibration peak (υC=O) of testosterone (Fig. 6a), proving the integration of T template molecules in the MIP polymer. This peak disappeared after washing and the peak characteristic of the υC=O vibration band of the acrylic polymer shifted to lower frequencies (1737 to 1732 $cm^{-1}$), confirming the existence of weak interactions between T template and the polymer matrix (Fig. 6c).

## 3.2. Electrical Effect of T Recognition and EIS Detection

CVs of the MIP sensor recorded at various T concentrations in presence of the ferro/ferricyanide redox probe are presented in Fig. 7. We can see that the intensity of iron probe oxidation and reduction peaks decreased when T concentration in equilibrium with the MIP film increased. The drop in charge transfer rate could be assigned to the decrease of available printed sites in MIP film that constitutes a conductive portion of the material [27].

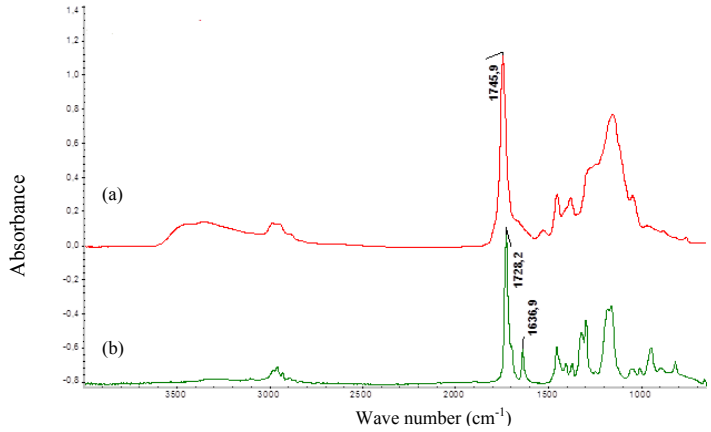


**Fig. 5.** FTIR spectra of the polymer NIP film (a) and the prepolymerization solution (b).

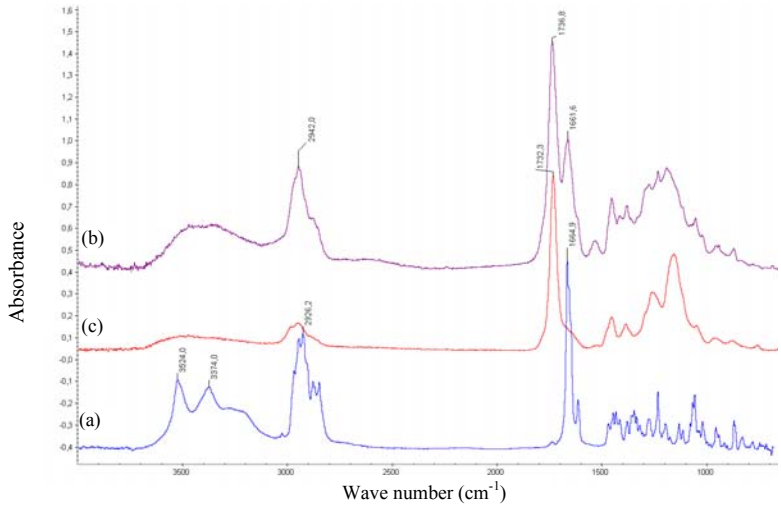


**Fig. 6.** FTIR spectra of testosterone (a) and of the MIP film before (b) and after (c) the washing step.

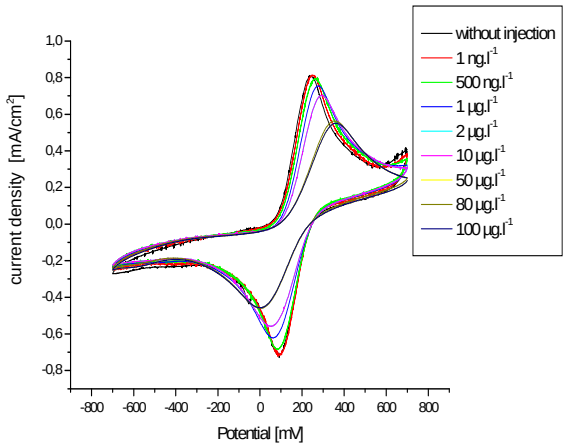


**Fig. 7.** Cyclic voltammograms of the testosterone-MIP sensor at various testosterone concentrations in 5 mM ferri/ferrocyanide PBS buffer solution. Scan speed 100 mV.s$^{-1}$.

Fig. 8 displays complex impedance spectra of the MIP sensor in contact with various T concentrations in the 1 ng.L$^{-1}$ to 100 µg.L$^{-1}$ range. They were all fitted with the classical Randles model, which enabled the calculation of $R_{ct}$ values, as previously done for Au, Au/SAM and Au/SAM/ACVA electrodes.

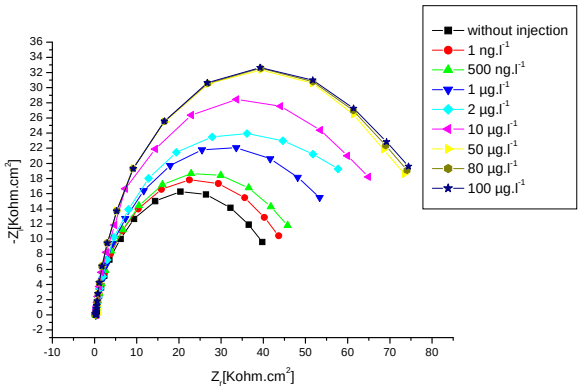


**Fig. 8.** Complex impedance spectra (Nyquist plots) of the MIP sensor at different testosterone concentrations. EIS measurements were performed at -400 mV in 5 mM ferro/ferricyanide PBS buffer.

Increasing T concentration resulted in an increase of $R_{ct}$ at the MIP-sensor/electrolyte interface (Fig. 9), in good agreement with cyclic voltammetry results. The MIP sensor response, expressed as the relative variation of $R_{ct}$, was linear up to 50 µg.L$^{-1}$ range, with a sensitivity of 0.28 per log C and a limit of detection of 103 ng.L$^{-1}$. When testosterone concentration exceeded 50 µg.L$^{-1}$, no additional variation of the response was observed, which could be attributed to the MIP printed sites saturation. As compared with the MIP, the NIP film response was very low and sensitivity to T concentration was only 0.016 per logC.

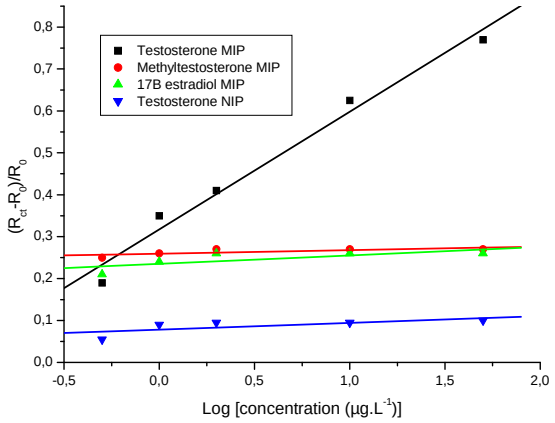


**Fig. 9.** Comparison of MIP and NIP sensors response towards testosterone and comparison with the methylstosterone and 17-β-estradiol MIP response. All measurements were performed in 5 mM of ferri/ferrocyanide PBS buffer solution, pH=7.5.

The label free electrochemical MIP sensor proposed in this work offers a large linear range and detection limit in the same order of magnitude than most of the T immunosensors already reported (Table 1).

**Table 1.** Comparison of analytical characteristics of the developed MIP sensor to those of some published electrochemical testosterone immunosensors.

| Receptor/ electrochemical probe | Linear range (ng.mL$^{-1}$) | Detection limit (pg.mL$^{-1}$) | Ref. |
|---|---|---|---|
| Antibody/HRP | 0.3-4 | 90 | [11] |
| Antibody/HRP | 0.005-50 | 1.7 | [5] |
| Antibody/HRP | 0.01-10 | 12.5 | [6] |
| Antibody/HRP | 0.1-10 | 85 | [17] |
| Antibody/Au nanowires | 1.2-83.5 | 100 | [7] |
| MIP/label free | 0.103-50 | 103 | This work |

The selectivity of the MIP-sensor was also tested by injecting endocrine disrupting compounds analogues (EDCs), i.e. methyltestosterone and 17-β estradiol. Sensitivities were 0.0085 and 0.020 per logC, respectively, representing only 3 % and 7 % of that obtained for T.

## 4. Conclusions

In this work, we proposed a novel impedimetric MIP sensor for T detection. MIP polymer was synthetized at the surface of gold electrodes via a photo-radical initiator covalently coupled to a self-assembled monolayer of amine terminated alkanethiol. The MIP sensor response was linear up to 50 µg.L$^{-1}$ ($R^2$=0.98312) with a limit of detection of 103 ng.L$^{-1}$. The selectivity towards other structurally

related EDCs (methyltestosterone and 17 β-estradiol) was very good, which is quite promising and paves the way for the elaboration of new sensors for EDCs determination.

## Acknowledgements

A. Betatache thanks Algerian and French government for PROFAS grant.

## References

[1]. World Anti-Doping Agency (WADA). The 2013 prohibited list-international standard. (http://www.wada-ama.org/Documents/World_Anti-Doping_Program/WADP-prohibited-list/2013/WADA-Prohibited-List-2013-EN.pdf) (accessed 26.02.2013)

[2]. M. Star-Weinstock, B. L. Williamson, S. Dey, S. Pillai, S. Purkayastha, LC-ESI-MS/MS analysis of testosterone at sub-picogram levels using a novel derivatization reagent, *Analytical Chemistry*, Vol. 84, 2012, pp. 9310-9317.

[3]. R. Zhang Shi, H. H. van Rossum, R. A. R. Bowen, Serum testosterone quantitation by liquid chromatography-tandem mass spectrometry: Interference from blood collection tubes, *Clin. Biochem.*, Vol. 45, 2012, pp.1706–1709.

[4]. T. Koal, D. Schmiederera, H. Pham-Tuan, C. Röhring, M. Rauh, Standardized LC–MS/MS based steroid hormone profile-analysis, *Journal Steroid Biochem. Mol. Biol.,* Vol. 129, 2012, pp. 129-138.

[5]. M. Eguílaz, M. Moreno-Guzman, S. Campuzano, A. Gonzalez-Cortes, P. Yanez-Sedeno, J. M. Pingarron, An electrochemical immunosensor for testosterone using functionalized magnetic beads and screen-printed carbon electrodes, *Journal Biosensors and Bioelectronics,* Vol. 26, 2010,pp. 517-522.

[6]. O. Laczka, F. J. del Campo, F. X. Munoz-Pascual, E. Baldrich. Electrochemical detection of testosterone by use of three-dimensional disc_ring microelectrode sensing platforms: application to doping monitoring, *Analytical Chemistry*, Vol. 83, 2011, pp. 4037-4044.

[7]. K.-Z. Liang, J.-S. Qi, W.-J. Mu, Z.-G. Chen, Biomolecules/gold nanowires-doped sol–gel film for label-free electrochemical immunoassay of testosterone, *Journal of Biochemical and Biophysical Methods,* Vol. 70, 2008, pp. 1156-1162.

[8]. R. M. Toledano, E.M.. Díaz-Plaza, J. M. Cortés, I. Blázquez, A. Vázquea, J. Villéna, J. Munoz-Guerra, Analysis of steroids in human urine by on line liquid chromatography–gas chromatography–mass spectrometry using the Through Oven Transfer Adsorption Desorption interface and a fraction collector, *Analytical Chemistry Acta,* Vol. 741, 2012, pp.78-85.

[9]. X. de la Torre, C. Colamonici, D. Curcio, F. Molaioni, F. Botrè, A comprehensive procedure based on gas chromatography–isotope ratio mass spectrometry following high performance liquid chromatography purification for the analysis of underivatized testosterone and its analogues in human urine, *Analytical Chemistry Acta,* Vol. 756, 2012, pp. 23-29.

[10]. M. Pole, W. Van Gansbeke, K. Deventer, P. Van Eenoo, Development of a sensitive GC-C-IRMS method for the analysis of androgens, *Biomedical Chromatography,* Vol. 27, 2013, pp. 259-266.

[11]. H. Lu, M. P. Kreuzer, K. Takkinen, G. G. Guilbault, A recombinant Fab fragment-based electrochemical immunosensor for the determination of testosterone in bovine urine, *Journal Biosensors and Bioelectronics*, Vol. 22, 2007, pp. 1756-1763.

[12]. N. I. K. Deshmukh, J. Barker, A. Petrocz, D. P. Naughton, Detection of testosterone and epitestosterone in human hair using liquid chromatography –tandem mass spectrometry, *Journal of Pharmaceutical and Biomedical Analysis*, Vol. 67–68, 2012, pp. 154–158.

[13]. H. Kataoka, K. Ehara, R. Yasuhara, K. Saito, Simultaneous determination of testosterone, cortisol, and dehydroepiandrosterone in saliva by stable isotope dilution on-line in-tube solid-phase microextraction coupled with liquid chromatography–tandem mass spectrometry, *Analytical Chemistry Bioanal.,* Vol. 405, 2013, pp. 331–340.

[14]. U. Turpeinen, E. Hämäläinen, M. Haanpää, L. Dunkel, Determination of salivary testosterone and androstendione by liquid chromatography–tandem mass spectrometry, *Clinica Chimica Acta.,* Vol. 413, 2012, pp. 594–599.

[15]. W. Rosner, R. J. Auchus, R. Azziz, P. M. Sluss, H. Raff. Utility, Limitations, and Pitfalls in Measuring Testosterone: An Endocrine Society Position Statement, *Journal of Clinical Endocrinology and Metabolism,* Vol. 92, 2007, pp. 405-413.

[16]. W. M. Wouter, H. N. Bui, J. ten Kate, P. P. C. A. Menheere, W. P. Oosterhuis, H. L. Vader, A. C. Heijboer, M. J. W. Janssen, Accuracy of first and second generation testosterone assays and improvement through sample extraction, *Clinica Chimica,* Vol. 58, 2012, pp. 1154-1156.

[17]. K. Inoue, P. Ferrante, Y. Hirano, T. Yasukawa, H. Shiku, T. Matsue, A competitive immunochromatographic assay for testosterone based on electrochemical detection, *Talanta*, Vol. 73, 2007, pp. 886-892.

[18]. G. Vasapollo, R. Del Sole, L. Mergola, M. R. Lazzoi, A. Scardino, S. Scorrano, G. Mele, Molecularly Imprinted Polymers: Present and Future Prospective *International Journal of Molecular Sciences,* Vol.12, 2011, pp. 5908- 5945.

[19]. Y. Fuchs, O. Soppera, K. Haupt, Photopolymerization and photostructuring of molecularly imprinted polymers for sensor applications—A review, *Analytical Chemistry Acta*, Vol. 717, 2012, pp. 7-20.

[20]. B. T. S. Bui, K. Haupt, Preparation and evaluation of a molecularly imprinted polymer for the selective recognition of testosterone—application to molecularly imprinted sorbent assays, *Journal of Molecular Recognition*, Vol. 24, 2011, pp. 1123-1129.

[21]. S. Mirmahdieh, A. Mardihallaj, Z. Hashemian, J. Razavizadeh, H. Ghaziaskar, T. Khayamian, Analysis of testosterone in human urine using molecularly imprinted solid-phase extraction and corona discharge ion mobility spectrometry, *Journal of Separation Science*, Vol.34, 2011, pp. 107–112.

[22]. I. Gavrilovic, K. Mitchell, A. D. Brailsford, D. A. Cowan, A. T. Kicman, R. J. Ansell, A molecularly

imprinted receptor for separation of testosterone and epitestosterone, based on a steroidal cross-linker, *Steroids*, Vol. 76, 2011, pp. 478-483.
[23]. K. RyAnne Noss, A. D. Vaughan, M. E. Byrne, Tailored Binding and Transport Parameters of Molecularly Imprinted Films via Macromolecular Structure: The Rational Design of Recognitive Polymers, *Journal of Applied Polymer Science*, Vol. 107, 2008, pp. 3435-3441.
[24]. C. He, F. Liu, K. Li, H. Liu, Molecularly imprinted polymer film grafted from porous silica for selective recognition of testosterone, *Journal Analytical Letters*, Vol. 39, 2006, pp. 275-286.
[25]. S. C. Huang, G. B. Lee, F. C. Chien, S. J. Chen, W. J. Chen, M. C. Yang. A microfluidic system with integrated molecular imprinting polymer films for surface plasmon resonance detection, *Journal of Micromechanics and Microengineering*, Vol. 16, 2006, pp. 1251-1257.
[26]. M. Lotierzo, O. Y. F. Henry, S. Piletsky, I. Tothill, D. Cullen, M. Kania, B. Hock, A. P. F Turner, Surface plasmon resonance sensor for domoic acid based on grafted imprinted polymer, *Biosensors and Bioelectronics*, Vol. 20, 2004, pp. 145-152.
[27]. P. Y. Chen, P. C. Nien, C. T. Wu, T. H. Wu, C. W. Lin, K. C. Ho. Fabrication of a molecularly imprinted polymer sensor by self-assembling monolayer/mediator system, *Analytical Chemistry Acta*, Vol. 643, 2009, pp. 38-44.

---